A study on some physical and mechanical properties of molded thermal insulation materials produced from perlite and boric acid added forestry by-products

Fatih Tuncay Efe

fatihtuncayefe@gmail.com

Çanakkale Onsekiz Mart University

Research Article

Keywords: Pine bark, pine cone, perlite, thermal insulation, mechanical properties

Posted Date: August 10th, 2022

DOI: https://doi.org/10.21203/rs.3.rs-1935639/v1

Additional Declarations: No competing interests reported.

Version of Record: A version of this preprint was published at Wood Material Science & Engineering on November 14th, 2022. See the published version at https://doi.org/10.1080/17480272.2022.2144761.

Abstract

Thousands of tons of bark and cones are produced each year in the forest products industry and the natural life cycle of forests. These raw materials are either burned or left in the forest. In both cases, it causes both environmental problems and a significant loss of economic potential. On the other hand, the demand for thermal insulation materials is increasing day by day, and more synthetic and fossil-based raw materials with negative environmental effects are consumed. In this study, some physical and mechanical properties of molded thermal insulation materials produced from natural raw materials were investigated experimentally. In this context, 15 types of sandwich panel materials containing honeycomb-shaped core were produced from pine (*Pinus brutia* Ten.) bark and cones. The mean moisture content, density, compressive strength, tensile strength perpendicular to the surface (Internal adhesion strength), tensile strength parallel to the surface (Tensile strength), and dimensional stability (width-length-thickness change) values of the materials were 10.600%, 269.717 kg/m^3, 0.493.06 N/mm^2, 0.011 N/mm^2, 0.150 N/mm^2 and − 0.156%, -0.054%, 0.942%, respectively. According to the results, it was determined that the increase in particle size and perlite ratio in the materials produced from the bark decreased the density. Moreover, it was found that the particle size-moisture content relationship and the perlite ratio-moisture content relationship varied in the materials containing bark and cones, that the mechanical properties were higher in the materials containing cones, and that the dimensional stability did not show a regular change.

1. Introduction

The envelope of a building significantly influences the surrounding microclimate, creates a boundary between the indoor and outdoor environment, and plays an important role, as it affects the thermal comfort and energy losses of occupants during use. Interest in environmental and energy issues has grown exponentially in recent years, and many international and national policies have been adopted to provide the planet with a more sustainable future (Schiavoni et al. 2016). Natural resources are often described as "renewable" or "non-renewable". Renewable resources are the ones that can be regularly renewed or harvested, such as wood and agricultural products, and can be renewed to any desired level as long as production conditions are suitable. Non-renewable resources are the ones that can only be harvested once. Most of these are significantly limited; it is usually expressed as a reserve (Berge 2009). Glass wool, rock wool, polyurethane foam, expanded polystyrene foam and extruded polystyrene foam are the most widely used artificial thermal insulation materials. They are produced from non-renewable resources, and their production process is difficult and requires expensive investment. They also have a lot of negative environmental effects during and after use (Cetiner and Shea 2018). Concerns about the consumption of energy resources, raw materials and excessive pollution have increased in recent years. Much more emphasis is placed on recycling and the use of non-toxic materials in many studies (Blanchet et al. 2000; Korjenic et al. 2011). Environmental awareness cannot be limited to energy saving only; minimum energy and resource use and minimum production pollution during the manufacture of insulation materials are also the issues to be considered (Berge 2009). There is a growing trend in the

world towards the importance of a livable environment. Parallel to this trend, interest in non-toxic, renewable, easy, cheap and abundant natural resources, such as bark (especially coniferous species), cones and lignocellulosic wastes, which are easy to produce, is increasing day by day (Efe 2022). The above-mentioned natural raw materials are still not industrially converted into high value-added products; they cause environmental pollution and are generally burned (Kain 2016). Forests produce tons of waste and by-products, such as bark and cones, every year. Of these, the bark is resistant to microorganisms, has low thermal conductivity, and is environmentally friendly (Kain et al. 2015), while cones, despite being a renewable fiber source, are also not used effectively (Buyuksari et al. 2010; Arrakhiz et al. 2013). According to the 2021 statistics of the Food and Agriculture Organization (FAO), it was reported that 1.398 billion cubic meters of coniferous wood and 2.572 billion cubic meters of non-coniferous wood were produced in 2019(FAO 2021). Taking into account that the tree contains 10% bark on average (Xing et al. 2007; Hoong et al. 2011), it can be stated that the annual potential usable bark volume is 397 million cubic meters. Huge amounts of bark from forest products industry activities are either thrown away or burned each year (Barbu 2011; Pásztory et al. 2016). On the other hand, it is not known how many pine cones appear in the world each year, except for the stone pine. However, given the current tree inventory, it can be estimated that they are in very large quantities. It was determined that many studies were performed on bark and cones in the literature. Sirisha (Khuntia and Biswas 2020), birch (Réh et al. 2021), beech (Bekhta et al. 2021), cork (Pinto et al. 2018; Andrzejewski et al. 2019; Amaro et al. 2020; Mirski et al. 2020), pine (Zhang et al. 2020; Borysiuk et al. 2021), red cedar (Chen and Yan 2018), walnut, chestnut, fir and spruce (Aydın İ., Demirkır C., Çolak S. 2010) species were investigated as a filler in the production of wood-based composites. One of the focus of attention in recent years is bark-based insulation materials. In this context, cork (La Rosa et al. 2014; Ferreira et al. 2016), pine (Kain et al. 2012; Tudor et al. 2020a), black locust (Pásztory et al. 2017), spruce (Tudor et al. 2020b), poplar (Tsalagkas et al. 2019; Busquets-Ferrer et al. 2021), larix (Kain et al. 2014, 2015, 2018), spruce, pine, birch (Holmberg et al. 2016), and eucalyptus (Wesolowski et al. 2014) were investigated. Pine cones, another non-wood forest product, are a good candidate raw material for various uses with their strong fibrous structure, high specific gravity, and chemical content different from wood and bark. Many studies were conducted on pine cones. It was determined that the use of cones in the production of chip material or medium density fiber material (MDF) adversely affected its mechanical properties (Ayrilmis et al. 2009; Buyuksari et al. 2010; Sahin and Arslan 2011). The effects of cone fiber or flour contained in some matrices, such as epoxy (Baştürk et al. 2015; Kolář et al. 2019), polypropylene (Arrakhiz et al. 2012), high-density polyethylene (HDPE) (Guo et al. 2019), and polycaprolactone (PCL) (Jha et al. 2018), were investigated. In summary, it is understood that studies on the performance of bark and cone as composite, filler, thermal insulation material and filter were carried out in the literature. Some researchers reported in their studies that the bark could be supplied in high amounts as a raw material compared to other bio-based insulating materials (Busquets-Ferrer et al. 2021), that the relationships between particle size, material density and thermal conductivity would be a good topic for research (Kain et al. 2015), that the fire behavior and water absorption of insulation materials needed to be investigated in further studies (La Rosa et al. 2014; Pásztory et al. 2017; Tsalagkas et al. 2019), and that it was necessary to work on different chip geometries (Blanchet et al. 2000). In addition, some researchers' recommendation that the strength and

mechanical properties of thermal insulation materials should also be investigated (La Rosa et al. 2014; Ferreira et al. 2016; Pásztory et al. 2016; Tsalagkas et al. 2019) emphasizes the importance of the subject. The materials produced in the literature research are either gap-free, completely filled or loose; so far, no research has been found on the production of bark- and/or cone-based thermal insulation materials using honeycomb molds. The aim of this study is to determine some physical and mechanical properties of the molded composite material produced from pine cone and bark using a different technique and to analyze the relationship of these properties with the particle size and perlite ratio of the raw materials in the material content. The gap ratio of the produced materials is about 55%. In order to determine the physical and mechanical properties and to show the relationships of these properties with the production parameters, 15 types of materials were produced. Cones and barks were used in three particle sizes as fine, medium and coarse. Paraffin, boric acid and expanded perlite were used as additives in varying proportions. The data obtained in the study is promising for scientists doing research in this field, for the sector representatives producing commercial building sheathing materials, for the evaluation of the relevant people, and for the natural wastes to be the subject of long-term projects in parallel with national and/or international policies.

2. Materials And Methods

The bark and cones of Calabrian Pine (*Pinus brutia* Ten.) were used as raw materials because Turkey's most widely distributed coniferous species (OGM 2013) has the thickest bark. The bark and cones were collected in Yenice district, Çanakkale province, Turkey. The raw materials were procured in July 2018 because in this month, the production of logs is common, the cones shed their seeds, and there is a fast-natural drying. In the production of materials, paraffin, boric acid, and expanded perlite were added to improve moisture and fire resistance, lightness and insulation properties. Urea-formaldehyde resin was used as glue. Perlite was obtained from Genper Expanded Perlite Industry Business Corporation in Kütahya, Turkey; boric acid was obtained from Forscher, Turkey; and paraffin and urea-formaldehyde resin were obtained from Kastamonu Integrated Wood Industry, and Trade Corporation Particleboard Plant, Balıkesir, Turkey. The technical properties of the urea-formaldehyde resin, boric acid, perlite and paraffin are given in Table 1 and Table 2.

Table 1
Technical features of perlite and boric acid. Table was adopted from Efe, (2022).

Chemical Content	Ratio (%)	Physical Features	
Perlite			
SiO_2	71–74	Color	White
Al_2O_3	12–14	Bulk Density	50–60 kg/m^3
K_2O	5–6	Moisture Content	Max. 1%
Na_2O	3–4	pH	6–8.5
MgO	0.10–0.20		
CaO	0.8-1.0		
Fe_2O_3	0.5-1		
TiO_2	0.09 – 0.012		
Boric Acid			
B_2O_3	56.25–56.80		
Equivalent H_3BO_3	99.9-100.89		
SO_4	300 ppm max.		
Cl	5 ppm max.		
Fe	4 ppm max.		

Table 2
Technical features of urea-formaldehyde and paraffin. Table was adopted from Efe, (2022).

Features	Urea formaldehyde	Paraffin
Solid Matter	65%	58–65%
Viscosity	301.1 cPs	10–100 cPs
Flow time	70.64 s	10–30 s
Density	1.285 g/cm^3	0.850–0.960 g/cm^3
pH	8.54	8–11
Gel time	37 s	-

A hammer mill with 6 mm and 9 mm aperture sieves, 24 crushing jaws and a 3 kW motor used in grinding raw materials, and an air-circulating drying oven that can be adjusted digitally up to 300°C were purchased from Doğangül Makine Company, Gaziantep, Turkey. Steel sieves with 0.5, 1, 2, 3, 4 and 5 mm openings were used manually in the classification of the raw materials. A honeycomb-shaped aluminum mold set, with 500 × 350 × 50 mm, was purchased from Alper Torna Company, Gaziantep, Turkey, to produce the core layers of all materials. The surface layers were produced in Kocayusuf Piton-KP-1 brand hydraulic press, which can reach 130°C and 200 bar. Some other equipment used in production were as follows; A curing oven adjustable up to 200°C; digital humidity and temperature meters; 3 hydraulic jacks, each with a lifting capacity of 5 tons; and a digital balance with a 40 kg capacity. The tests were carried out in the Çanakkale Onsekiz Mart University Yenice Vocational School Forestry Department laboratory and Kahramanmaraş Sütçü İmam University Forestry Faculty laboratories.

2.1. Production of materials

The materials were produced in three stages: the production of 4 mm thick surface layers, the production of 32 mm thick core layers, and the assembly of the material. Material types and contents are shown in Table 3.

Table 3
Contents of boards. Table was adopted from Efe, (2022).

Materials	Content	Ratio (%)	Particle Size (PS) (mm)
A1	Bark	100	1 < PS < 2
A2		100	2 < PS < 3
A3		100	3 < PS < 4
B1	Cone	100	1 < PS < 2
B2		100	2 < PS < 3
B3		100	3 < PS < 4
C1	Bark/Cone	75/25*	2 < PS < 3
C2		50/50*	
C3		25/75*	
D1	Bark/Perlite	90/10#	2 < PS < 3
D2		80/20#	
D3		70/30#	
E1	Cone/Perlite	90/10#	2 < PS < 3
E2		80/20#	
E3		70/30#	

*: *By total material weight*, #: *By total material volume.*

In the production of all materials, 10% glue, 1% boric acid and 0.5% paraffin were used by weight. Cones and barks having air dry (12%-15%) moisture content were first ground in a hammer mill and then sieved by hand, and particles smaller than 1 mm and larger than 4 mm were removed as unused raw materials. Finally, it was dried in the oven until it reached 1%-2% moisture. In the production of the surface layers, a frame made of medium density fiberboard (MDF) with 20 × 450 × 550 mm as a template was used. Cone/bark, perlite, glue, boric acid and paraffin in varying proportions for each material were mixed with a hand mixer and laid in the template. Thus, material mats were created. Surface layer mats were pre-compressed with an 18 mm thick MDF material using 4 joiner's clamps. Finally, 4 mm thick materials were produced in a hydraulic press using a compression ratio of 1:5. In the production of the surface layers, 200 bar pressure was applied at 130°C for 8 minutes. The mixture of the same content as the surface layers was used in the production of the core layers. Here, the mixture was laid in a honeycomb-shaped aluminum mold, the voids of the material were removed by vibration, and 2 kg/cm^2 pressure was applied with hydraulic jacks. The mold was fixed under pressure and cured at 160°C for 30 minutes,

resulting in a 32 mm thick middle layer. The apparatus for the production of the honeycomb-shaped aluminum mold and the middle layer is shown in Figs. 1 and 2, respectively.

By bonding the surface layers to both sides of the core layer, the target material in the form of a 40 mm thick sandwich was produced. In this final stage, the pressing parameters were 130°C, 20 bar and 8 min.

2.1.1. Tests

2.1.1.1. Moisture content

TS EN 322 (1999a) standard was used to determine the moisture content. Four samples of 50 × 50 × 40 mm from each material were weighed first, the initial weight was recorded, and then they were kept in an oven at 103 ± 2°C until they reached the constant weight, and were weighed again. The moisture content was calculated according to the formula (1).

$$H = \frac{m_H - m_0}{m_0} x100$$

1

where H (%) is the moisture content, m_H (g) is the moist weight, and m_0 (g) is the dry weight.

2.1.1.2. Density

The density determination was performed according to TS EN 323 (1999b). Firstly, the samples were conditioned at 50 ± 5% RH and 23 ± 2°C. Specimens, 4 of each board type, with dimensions of 165 × 165 × 40 mm were used in the test.

2.1.1.3. Compressive strength (CS)

This test was carried out in accordance with TS EN 826. The dimensions of 4 samples for each material were 165 x 165 x 40 mm. The test was performed after the samples were conditioned for at least 6 hours at (23 ± 5) °C. In this test, the compressive strength of the material was calculated by the formula (2), and the compressive stress corresponding to 10% strain was calculated by the formula (3).

$$\sigma_m = 10^3 \frac{F_m}{A_0}$$

2

where σ_m is the compressive strength (kPa), σ_{10} is the compressive stress corresponding to 10% strain (kPa), F_m is the maximum force (N), A_0 is the initial cross-sectional area of the sample (mm^2).

$$\sigma_{10} = 10^3 \frac{F_{10}}{A_0}$$

3

where F_{10} is the force (N) corresponding to 10% strain, and A_0 is the initial cross-sectional area (mm^2) of the test specimen.

2.1.1.4. Tensile strength perpendicular to the surface (IB)

This test was carried out in the Kahramanmaraş Sütçü İmam University Forestry Faculty Forest Industrial Engineering laboratories in accordance with TS EN 1607. The samples were conditioned at 50 ± 5% relative humidity and 23 ± 2°C, and the experiment was carried out in this environment. The test was carried out on the Zwick Roel universal Z010 machine at a loading speed of 10 mm/min. Preloading was not applied to the samples. The IB was calculated by determining the maximum force at break (MPa). Five samples of 50 x 50 x 40 mm were used for each type of material. The IB was calculated with the help of formula (4).

$$\sigma_m \frac{F_m}{A} = \frac{F_m}{lxb}$$

4

where σ_m is the IB (kPa), F_m is the maximum tensile force (kN), A is the cross-sectional area of the sample (m^2), l,b is the length, and width of the sample (m).

2.1.1.5. Tensile strength parallel to the surface (TS)

This test was carried out in the Kahramanmaraş Sütçü İmam University Forestry Faculty Forest Industrial Engineering laboratories in accordance with TS EN 1608. The samples were conditioned at 50 ± 5% relative humidity and 23 ± 2°C, and the experiment was carried out in this environment. In the test, ALSA brand hydraulic test device with a capacity of 50 kN was used. Three samples were used for each type of material in the test. Sample sizes were adapted because the dimensions of the materials were not large enough. The TS was calculated as kPa according to the Eq. (5). Figure 3 shows the test setup.

$$\sigma_T \frac{F_m}{dxb}$$

5

where σ_T is TS (kPa), F_m is the maximum tensile force (kN), d is the thickness of the test area (m), and b is the width of the test area (m).

2.1.1.6. Dimensional stability (DS)

This test was carried out in the Kahramanmaraş Sütçü İmam University Forestry Faculty Forest Industrial Engineering laboratories in accordance with TS EN 1604. The test was carried out in a NUVE brand TK120 model air-conditioning cabinet at 50 ± 5% relative humidity and 23 ± 2°C. Two samples of 227 x

227 x 40 mm were used from each material. According to the standard, initially three measurements were taken from the width and length of the samples (l_{01}, l_{02}, l_{03}, b_{01}, b_{02}, b_{03}), and the thickness was recorded from five different points (d_{01}, d_{02}, d_{03}, d_{04}, d_{05}). After the initial dimensions of the samples were measured with an accuracy of 0.1 mm, they were placed in the air-conditioning cabinet. It was removed after 48 hours and kept at 50 ± 5% relative humidity and 23 ± 2°C for at least 3 hours, and then the sample sizes (*lt, bt, dt*) were measured again. Final measurements were made for the initial measurement points (l_{t1}, l_{t2}, l_{t3} and b_{t1}, b_{t2}, b_{t3} and d_{t1}, d_{t2}, d_{t3}, d_{t4}, d_{t5}). The size changes $\Delta\varepsilon_l$, $\Delta\varepsilon_b$ and $\Delta\varepsilon_d$ in the samples were calculated with the equations (6), (7), and (8).

$$\Delta\epsilon_l = 100x\frac{lt - l_0}{l_0}$$

6

$$\Delta\epsilon_b = 100x\frac{bt - b_0}{b_0}$$

7

$$\Delta\epsilon_d = 100x\frac{dt - d_0}{d_0}$$

8

where $\Delta\varepsilon l$ is the length change (%), $\Delta\varepsilon b$ is the width change (%), $\Delta\varepsilon d$ is the thickness change (%), l_0, b_0, d_0 are the initial dimensions (mm), and l_t, b_t, d_t are the final dimensions (mm).

3. Results And Discussion

Some of the physical and mechanical properties of the materials are shown in Table 4. The relations of the data in this table with each other were also examined with graphics.

Table 4 Some physical and mechanical properties of the materials.

Materials	Physical and mechanical properties							
	MC (%)	ρ (kg/m^3)	σ_{10} (N/mm^2)	σ_m (N/mm^2)	σ_T (N/mm^2)	Dimensional stability (DS)		
						$\Delta\varepsilon_l$ (%)	$\Delta\varepsilon_b$ (%)	$\Delta\varepsilon_d$ (%)
A1	10.40 (0.20) *	273.113 (11.06)	0.266 (0.03)	0.0027 (0.00)	0.1498 (0.01)	-0.203 (0.13)	0.086 (0.22)	2.897 (0.81)
A2	10.42 (0.15)	257.228 (2.19)	0.304 (0.01)	0.0129 (0.03)	0.1318 (0.01)	-0.393 (0.11)	-0.136 (0.02)	1.042 (0.15)
A3	11.29 (0.31)	262.334 (2.58)	0.349 (0.01)	0.0095 (0.07)	0.0756 (0.04)	-0.101 (0.01)	-0.132 (0.16)	-0.067 (0.21)
B1	11.99 (0.10)	305.425 (2.40)	0.793 (0.05)	0.0258 (0.00)	0.3046 (0.01)	-0.167 (0.04)	0.044 (0.09)	0.632 (2.31)
B2	10.79 (0.32)	292.223 (10.65)	0.722 (0.02)	0.0221 (0.01)	0.1793 (0.02)	-0.163 (0.10)	-0.108 (0.05)	5.180 (0.23)
B3	10.50 (0.36)	298.378 (6.10)	0.891 (0.02)	0.0220 (0.02)	0.2162 (0.01)	-0.107 (0.25)	0.335 (0.10)	1.716 (2.59)
C1	10.32 (0.16)	263.370 (9.79)	0.364 (0.04)	0.0061 (0.00)	0.1473 (0.02)	-0.217 (0.08)	-0.258 (0.16)	-0.838 (0.66)
C2	11.62 (1.79)	252.695 (10.07)	0.324 (0.02)	0.0068 (0.00)	0.1693 (0.02)	-0.112 (0.03)	-0.079 (0.04)	2.416 (0.44)
C3	10.33 (0.09)	244.485 (3.84)	0.315 (0.01)	0.0057 (0.00)	0.0681 (0.00)	-0.103 (0.10)	-0.042 (0.09)	1.837 (3.01)
D1	8.92 (2.04)	261.286 (8.18)	0.310 (0.02)	0.0082 (0.00)	0.1315 (0.01)	-0.156 (0.05)	0.028 (0.24)	2.039 (2.24)
D2	9.59 (0.26)	261.574 (9.61)	0.328 (0.03)	0.0045 (0.00)	0.1403 (0.00)	-0.116 (0.00)	-0.221 (0.04)	0.184 (0.82)
D3	9.81 (0.66)	259.875 (6.68)	0.414 (0.03)	0.0093 (0.00)	0.0897 (0.03)	-0.090 (0.03)	-0.145 (0.11)	-0.730 (1.20)
E1	15.96 (3.48)	275.383 (10.31)	0.739 (0.11)	0.0117 (0.01)	0.2098 (0.03)	-0.075 (0.06)	-0.055 (0.04)	1.800 (0.10)
E2	9.96 (0.07)	272.094 (9.10)	0.709 (0.03)	0.0089 (0.01)	0.1279 (0.01)	-0.007 (0.31)	-0.088 (0.10)	-4.413 (1.25)
E3	7.10 (0.51)	266.287 (10.06)	0.563 (0.05)	0.0026 (0.00)	0.1048 (0.01)	-0.327 (0.01)	-0.042 (0.13)	0.431 (1.11)

** Values in brackets are standard deviations.*

3.1 Moisture content (MC)

The MC of the materials was in the range of 7.10%-15.96% (Table 4). The mean MC of all materials was 10.60% with a standard deviation of 1.82%. As seen in Fig. 4, the MC values changed in direct proportion to particle size in the 100% bark-based group A materials and inversely in the 100% cone-based group B materials. The variation of the MC values in the perlite containing materials is shown in Fig. 5. It was determined that the perlite ratio had an effect that increased the MC in the D group materials and decreased it in the E group materials. It was observed that perlite did not have the same effect in both groups due to the structural differences of the bark and the cone. The samples containing perlite were expected to have higher MC than the others. However, except for E1, the MC values of the D and E group samples were lower. This can be explained by the increased density of perlite under pressure and the decrease in hygroscopicity. Kain et al. (2012, 2013b) produced materials with particle sizes between 0-45 mm from pine (*Pinus sylvestris*) bark, and found a mean MC of 12.2% with a standard deviation of 0.6%. The MC of 20 mm thick boards produced from Larch (*Larix decidua* Mill.) bark was reported to be 15.6% with a standard deviation of 0.7% (Kain et al. 2015). Tsalagkas et al. (2019) found the MC of the boards produced from poplar (*Populus* sp.) bark was in the range of 7.29%-9.12%. Materials produced from 19–25.4 mm thick larch and poplar bark were reported to have MC in the range of 3%-8.6% (Tudor et al. 2020b). On the other hand, the MC of 19-21 mm thick materials produced from bark of spruce (*Picea abies* L.) and larch (*Larix decidua* Mill.) was reported to be 8%-9% (Tudor et al. 2020a). In general, although the MC results obtained in this study were similar to some of the studies mentioned above, there were differences in terms of wood type, raw material particle size, pressing technique, board form, other materials added to the board, and board thickness.

3.2 Density

Density has a significant effect on many properties of the material, such as water absorption, bending strength, and thermal insulation performance (Xing et al. 2007; Gupta et al.2011). The lowest and highest densities of the materials were 244.48 kg/m^3 in the C3 group and 305.43 kg/m^3 in the B1 group, respectively. The mean density was 269.70 kg/m^3 with a standard deviation of 16.50. In this study, it was observed that the densities of the materials were affected by the structural properties such as raw material density, fiber, extractive substance, etc., and production parameters such as gluing, laying, additives, and compression ratio. In this context, although the expected results were obtained in some of the materials; some were not available.

It is thought that the density differences are due to the different resistance of bark and cones with different particle sizes under pressure. Figs. 6 and 7 give clues about density-particle size and density-perlite ratio relationships. Table 4 shows that there was a regular variation depending on the bark/cone mixture in the group C samples and depending on the cone/perlite mixture in the group E samples. However, in the other groups, it was observed that the density results did not have a regular variation depending on the content. It was expected that there would be an inverse proportion between particle size and material density in the group A and B samples, but it was seen that there was no such relationship. The main reasons leading to this situation are considered as non-homogeneous internal adhesion, laying and pressing errors. The density of the cone particles was higher than that of the bark.

Therefore, a higher density was measured in the B and E group materials than the others due to the cone content. The group D samples consisting of shell-perlite mixture were expected to have the lowest density, but it was determined that it was not so due to the possible errors mentioned above. In general, it is preferred that the densities of insulation materials are low (ρ=10-1000 kg/m^3) because the main factor that makes the insulation is the air gaps in the material. In other words, the thermal insulation properties of materials with low unit volume weights are better than materials with higher unit volume weights (Akıncı 2007). Studies with similar raw materials were examined in the literature. For example, the densities of 20 mm thick materials produced from 6-10 mm thick larch (*Larix decidua* Mill.) bark were between 270-540 kg/m^3 (Kain et al. 2014), the densities of 20 mm thick boards produced from the bark and woods of *Picea abies*, *Pinus sylvestris*, and *Abies alba* were between 350-500 kg/m^3 (Kain et al. 2013a), the densities of 10-20-30-40 mm thick boards produced from 1-8 mm, 8-13 mm and 13-45 mm black locust (*Robinia pseudoacacia*) barks were between 185.8-548.3 kg/m^3 (Pásztory et al. 2017), and the densities of 30 mm thick materials produced from the 3-6 mm and 10-30 mm particles of larch (*Larix decidua* Mill.) barks were found to be between 191-609 kg/m^3 (Kain et al. 2018). Moreover, the densities of 10 mm thick boards produced using stone pine (*Pinus pinea* L.) cones were between 730-760 kg/m^3 (Ayrilmis et al. 2009), and the densities of 20 mm thick materials produced using poplar (*Populus* sp.) bark were 336.80-413.07 kg/m^3 (Tsalagkas et al. 2019), and the mean densities of the boards produced with pine and larch bark were reported to be 960 kg/m^3 (Rudenko 2010). When the densities of the materials in the above studies were compared with the data in this study, it was seen that the mean density was 269.717 kg/m^3 and that the change interval of 244.485-305.430 kg/m^3 was considerably lower than them.

3.3 Mechanical properties

There is a need for thermal insulation materials with sufficient compressive strength in horizontal or slightly inclined applications in buildings. If the thermal insulation material does not have sufficient compressive strength, the material will be deformed against the forces acting on it from the external environment and will not be able to fulfill the task expected from it (Akıncı 2007). One of the important features of thermal insulation materials is the mechanical resistance they show against loads of variable duration. In thermal insulation materials, a decrease in the thickness of more than a certain value causes an unacceptable deterioration in the performance of the material. At this time, even if the material carries a load, it cannot fulfill its main task. For this reason, in thermal insulation materials, the compressive stress at 10% deformation (that is when there is a 10% decrease in thickness) is taken as the basis. This value is called compressive stress at 10% deformation, and is shown by σ_{10}. The highest compressive strength was measured with 0.891 N/mm^2 in the B3 group material, and the lowest compressive strength was measured in the A1 group material with 0.266 N/mm^2 (Table 4). The mean compressive strength value was found to be 0.493 N/mm^2 with a standard deviation of 0.21. On the other hand, the highest values were recorded in the B and E group materials containing cones. It is considered that the main reasons for this variability in the data were the density differences of the raw materials (the average bulk

density of the bark was 210-220 kg/m^3 and the average bulk density of the cone was 220-270 kg/m^3) and structural differences. In addition, the possible reason for the low compressive resistance of the perlite-containing groups may be that perlite and the other raw materials could not provide good internal bonding. On the other hand, the compressive strength increased in direct proportion to the particle size in the group A materials and in direct proportion to the perlite ratio in the group D materials. It decreased inversely with the perlite ratio in the E group materials and inversely with the cone ratio in the C group materials. No regular change was observed in the B group materials. Fig. 8 shows the particle size-density-compressive strength relationships. The general expectation is that the compressive strength increases with the increase in density. However, the findings show that there was no such a relationship between density and compressive strength; however, it showed that the particle size increase had a positive effect on the compressive strength. It is thought that gluing and pressing errors had an effect on the results, especially in the production of core layers.

Fig. 9 gives an idea about the perlite ratio-density-compressive strength relationships. As the perlite ratio increased in the D group materials containing shell, the compressive strength increased, while it decreased in the E group materials containing cones. It was determined that the compressive strength changed inversely with the density of the group D materials and directly proportional to the density of the group E materials. Fig. 10 shows the behavior of the group A materials in the compressive resistance test. According to the graph, the maximum deformation of the A1, A2 and A3 group materials occurred at the end of the application of force of 4.92 N, 7.53 N and 9.32 N, respectively. These results showed that the compressive strength increased as the particle size increased.

Fig. 11 shows the behavior of the group B materials in the compressive resistance test. According to the graph, the maximum deformation of the B1, B2 and B3 group materials occurred at the end of the application of force of 20.15 N, 17.61 N and 24.83 N, respectively. These results showed that there was an irregular relationship between particle size and compressive strength in the group B materials. Fig. 12 shows the behavior of the group C materials in the compressive resistance test. According to the graph, the maximum deformation of the C1, C2 and C3 group materials occurred at the end of the force application of 14.38 N, 10.01 N and 8.60 N, respectively. These results showed that the compressive strength of C group materials decreased as the shell ratio decreased.

Fig. 13 shows the behavior of the group D materials in the compressive strength test. According to the graph, the maximum deformation of the D1, D2 and D3 group materials occurred at the end of the force application of 14.87 N, 9.15 N and 12.20 N, respectively. These results showed that although there was no linear relationship between the perlite content and the compressive strength in the group D materials, the general trend was that the perlite ratio decreased the compressive strength. Fig. 14 shows the behavior of the group E materials in the compressive strength test. According to the graph, the maximum deformation of the E1, E2 and E3 group materials occurred at the end of the application of force of 19.34 N, 19.58 N and 14.90 N, respectively. These results showed that although there was no linear relationship between the perlite content and the compressive strength in the group E materials, the general trend was that the perlite ratio increased the compressive strength.

The force-deformation graphs showed that in general, all materials underwent a similar plastic deformation from the beginning of the test up to 2 N, and that after this point, a permanent deformation took place. In summary, the group A, C and D materials containing shells had lower compressive strength than the others; the group B materials showed the highest compressive strength; and the perlite content had a different effect depending on whether the raw material was bark or cone. It was determined that the structural properties and production parameters of the bark and cone also affected the compressive strength. The compressive stress/strength of mineral wools at 10% deformation, which is one of the materials currently widely used in the insulation sector, is given between 0.5-500 kPa in TS EN 13162+A1. The compressive stress at 10% deformation for EPS is given as 30-500 kPa in TS EN 13163:2012+A2, and the compressive stress/strength of XPS at 10% deformation is given as 100-1000 kPa in TS EN 13164+A1. According to EN 13171:2012, the compressive stress at 10% deformation required by wood fiber thermal insulation boards was reported between 5-500 kPa. The compressive strength data at 10% deformation of all material groups produced in this study met the requirements in the standards given above. (Kain et al. 2012, 2013b) reported that the panel density showed a highly significant ($p<0.001$) positive correlation with CR and some other mechanical properties (Dost 1971; Kain et al. 2012). It was reported that the increase in density did not directly affect the mechanical properties (Gupta et al. 2011), and that the mechanical properties of shell-based materials produced in different particle sizes weakened as the particle size increased (Kain et al. 2012). In addition to the particle size, which determines the density on mechanical properties, the glue ratio, gluing, and pressing conditions should not be ignored. Giannotas et al. (2022) measured the CRs of the composites produced from cement and Scots pine (*Pinus sylvestris* L.) and black pine (*Pinus nigra* L.) shells between 4.15-17.77 N/mm^2, and they reported that the CR ratio decreased as the content of bark increased. In a study, the composites of different densities were produced using gypsum, cork (*Quercus suber*) and sawdust, and CRs were found between 2.27-6.58 N/mm^2. It was reported that there was an improvement in compressive strength values in parallel with the increase in density (Hernández-Olivares et al. 1999). IB and TS are the mechanical properties that are expected to meet the standards in thermal insulation materials. These properties give clues as to whether the components that make up the material are sufficiently bonded to each other, and thus whether the integrity of the material can be maintained for long periods of time during use. On the other hand, it is important that the material maintains its dimensional stability during storage, transportation, and in variable environmental conditions (temperature, humidity, wind, etc.) at the place of use. Otherwise, undesirable effects, such as surface blistering, fluctuations, and pulling back of fasteners, may occur.

According to Figs. 15 and 16, the TS of the group A, B, D and E materials was higher than IB. The results are expected to be like this due to the hollow structure of the materials, the shape of the specimens in the IB and TS tests, and the test mechanisms. The IB and TS of the group B materials were higher than those of the group A materials. This result was given by the fibrous structure of the cones that made up the B group materials and thus a stronger bonding in gluing. The TS of the group A materials decreased as the particle size increased, whereas the IBs did not show a regular variation. While the TSs of the group B materials were expected to decrease in parallel with the increase in particle size, it was observed that

there was no regular decrease. This result is thought to be caused by some deficiencies or errors in the production stages. The IBs of the B group materials were very close to each other. The TS of the D group materials was lower than that of the E group materials. It was found that as the perlite ratio in the material content increased, the TS values generally decreased and that the IB values were independent of these ratios. The IB values of the three-layer MDF with a density of 850 kg/m^3 produced using black spruce bark in the middle layer were measured between 0.37-0.58 N/mm^2 (Xing et al. 2007). (Kainet al. 2015) determined the IBs of the composite materials produced from larch shells at densities of 500-450-400-350-300-250 kg/m^3 between 0.32-0.06 N/mm^2. Particle boards were produced by using the bark of black spruce (*Picea mariana* (Mill.)) and trembling aspen (*Populus tremuloides* (Michx.)) in fine, medium and coarse grain sizes. It was determined that the mechanical properties weakened as the bark ratio increased, and that the materials with fine bark grain size showed higher IB (Yemele et al. 2008b, a). In addition, the IB values of the particle boards produced by (Buyuksari et al. 2010) with pine (*Pinus nigra* Arnold var. *pallasiana*) and beech (*Fagus orientalis* Lipsky) wood and pine (*Pinus pinea* L.) cones were between 0.29-0.57 N/mm^2, and it was stated that as the cone ratio of the boards increased, the IB values decreased. In some studies, the bending and breaking strengths of composite materials produced using Polycaprolactone (CAPA 6800) pine (*Pinus pinea* L.) cones were inversely proportional to the cone ratio (Jha et al. 2018), and the mechanical properties of composites produced from polypropylene and pine (*Pinus pinea* L.) cones improved with the increase in cone ratio (Arrakhiz et al. 2012). In this study, the dimensional change results of the materials were found to be -0.156% ($\Delta\varepsilon l$), -0.054% ($\Delta\varepsilon b$) and 0.942% ($\Delta\varepsilon d$). The maximum and minimum $\Delta\varepsilon l$ values were -0.007% and -0.393% in the E2 and A2 groups; the maximum and minimum $\Delta\varepsilon b$ values were 0.335% and -0.258% in the B3 and C1 groups, and the maximum and minimum $\Delta\varepsilon d$ values were 5.180% and -4.413% in the B2 and E2 groups, respectively. As can be seen in the findings, the dimensional changes of the materials occurred at reasonable rates, and the dimensional stability data in terms of width and length gave better results than thickness. As possible reasons for the differences, it can be suggested that the free-falling particles in the laying phase generally overlap in the horizontal position and provide better bonding, and that especially the pressure applied in the production of the middle layer is lower than that of the surface layers.

4. Conclusion

In this study, some physical and mechanical properties of bio-based composite materials produced from tree bark and cones with added perlite and boric acid were investigated. The materials produced were different from the materials in the literature both in content and design. Therefore, it was determined that some of the physical and mechanical properties found were quite different from previous studies, and that some were similar. The data obtained in this research is promising in terms of being remarkable for many people related to the subject, especially for scientists and sector representatives producing building thermal insulation materials, and in terms of natural wastes being the subject of long-term projects in parallel with national and/or international policies. In general, the following can be stated:

- The fact that the material has 55% void has significantly reduced its density.

- As the particle size and the perlite ratio increased in the bark-based materials, the density of the material decreased.
- The particle size-MC relationship and the perlite ratio-MC relationship varied in the materials containing bark and cones. It can be thought that this is due to the structure of the bark and cone.
- It was found that the mechanical properties were better in the cone-based materials, that the dimensional stability did not show a regular change, and that each material group was, however, more sensitive in the thickness direction.

As a result, by changing the bark and cone form, they can be converted into composite materials with increased thermal insulation and mechanical properties. In further studies, the materials to be produced will be able to show better insulation and mechanical properties by thinning the honeycomb walls and surface layers in the material design.

Declarations

Acknowledgements

I would like to thank Prof. Dr. Bekir Cihad BAL, Assoc. Prof. Dr. Ertuğrul ALTUNTAŞ and Assoc. Prof. Dr. Kadir KARAKUŞ for their valuable supports.

Funding

This research was supported by the Scientific and Technological Research Council of Turkey (TUBITAK) (Project Number: 217O356).

Conflict of interest: The corresponding author states that there is no conflict of interest.

References

1. Akıncı H (2007) Today’s thermal insulation materials applied, their properties, application techniques, and cost analyses. Master's thesis, institute of natural sciences, department of structural sciences Sakarya University
2. Amaro AM, Reis PNB, Ivañez I et al (2020) The high-velocity impact behaviour of kevlar composite laminates filled with cork powder. Appl Sci 10:1–12. https://doi.org/10.3390/app10176108
3. Andrzejewski J, Szostak M, Barczewski M, Łuczak P (2019) Cork-wood hybrid filler system for polypropylene and poly(lactic acid) based injection molded composites. Structure evaluation and mechanical performance. Compos Part B Eng 163:655–668. https://doi.org/10.1016/j.compositesb.2018.12.109
4. Arrakhiz FZ, Benmoussa K, Bouhfid R, Qaiss A (2013) Pine cone fiber/clay hybrid composite: Mechanical and thermal properties. Mater Des 50:376–381. https://doi.org/10.1016/j.matdes.2013.03.033

5. Arrakhiz FZ, El Achaby M, Benmoussa K et al (2012) Evaluation of mechanical and thermal properties of Pine cone fibers reinforced compatibilized polypropylene. Mater Des 40:528–535. https://doi.org/10.1016/j.matdes.2012.04.032
6. Aydın İ, Demirkır C, Çolak S(2010) III. National Black Sea Forestry Congress. Eval Flours Differ Wood Barks as FıllerPlywood Panels1825–1833
7. Ayrilmis N, Buyuksari U, Avci E, Koc E (2009) Utilization of pine (Pinus pinea L.) cone in manufacture of wood based composite. For Ecol Manage 259:65–70. https://doi.org/10.1016/j.foreco.2009.09.043
8. Barbu MC (2011) Current Developments In The Forestry And Wood Industry. Pro Ligno 8:89–99
9. Baştürk SB, Kürşat K, P İ, Y. Y (2015) Mechanical Properties of Acorn and Pine Cone Filled Polymer Composites. Am Sci Res J Eng Technol Sci 14:144–153
10. Bekhta P, Sedliačik J, Noshchenko G et al (2021) Characteristics of beech bark and its effect on properties of UF adhesive and on bonding strength and formaldehyde emission of plywood panels. Eur J Wood Wood Prod 79:423–433. https://doi.org/10.1007/s00107-020-01632-8
11. Berge B (2009) The Ecology of Building Materials, Second. Architectural Press, Oxford, UK
12. Blanchet P, Cloutier A, Riedl B (2000) Particleboard made from hammer milled black spruce bark residues. Wood Sci Technol 34:11–19. https://doi.org/10.1007/s002260050003
13. Borysiuk P, Boruszewski P, Auriga R et al (2021) Influence of a bark-filler on the properties of PLA biocomposites. J Mater Sci 56:9196–9208. https://doi.org/10.1007/s10853-021-05901-6
14. Busquets-Ferrer M, Czabany I, Vay O et al (2021) Alkali-extracted tree bark for efficient bio-based thermal insulation. Constr Build Mater 271:121577. https://doi.org/10.1016/j.conbuildmat.2020.121577
15. Buyuksari U, Ayrilmis N, Avci E, Koc E (2010) Evaluation of the physical, mechanical properties and formaldehyde emission of particleboard manufactured from waste stone pine (Pinus pinea L.) cones. Bioresour Technol 101:255–259. https://doi.org/10.1016/j.biortech.2009.08.038
16. Cetiner I, Shea AD (2018) Wood waste as an alternative thermal insulation for buildings. Energy Build 168:374–384. https://doi.org/10.1016/j.enbuild.2018.03.019
17. Chen H, Yan N (2018) Application of Western red cedar (Thuja plicata) tree bark as a functional filler in pMDI wood adhesives. Ind Crops Prod 113:1–9. https://doi.org/10.1016/j.indcrop.2018.01.005
18. Dost W (1971) Redwood bark fiber in particleboard. For Prod J 21:38–43
19. Efe FT (2022) Investigation of some physical and thermal insulation properties of honeycomb-designed panels produced from Calabrian pine bark and cones. Eur J Wood Wood Prod 80:705–718. https://doi.org/10.1007/s00107-021-01781-4
20. FAO (Food and Agriculture Organization of The United (2021) No Title. http://www.fao.org/faostat/en/#data/FO. Accessed 21 May 2021
21. Ferreira R, Pereira D, Gago A, Proença J (2016) Experimental characterisation of cork agglomerate core sandwich panels for wall assemblies in buildings. J Build Eng 5:194–210.

https://doi.org/10.1016/j.jobe.2016.01.003

22. Giannotas G, Kamperidou V, Stefanidou M et al (2022) Utilization of tree-bark in cement pastes. J Build Eng 57:104913. https://doi.org/10.1016/j.jobe.2022.104913
23. Guo Y, Liu D, Chen Y et al (2019) Preparation and properties of carbon-fiber- and pine-cone-fiber-reinforced high-density polyethylene composites. J Appl Polym Sci 136:1–7. https://doi.org/10.1002/app.47304
24. Gupta G, Yan NFMW (2011) Effects of Pressing Temperature and Particle Size on Bark Board Properties Made from Beetle-Infested Lodgepole Pine (Pinus contorta) Barks. For Prod J 61:478–488. https://doi.org/https://doi.org/10.13073/0015-7473-61.6.478
25. Hernández-Olivares F, Bollati MR, Del Rio M, Parga-Landa B (1999) Development of cork-gypsum composites for building applications. Constr Build Mater 13:179–186. https://doi.org/10.1016/S0950-0618(99)00021-5
26. Holmberg A, Wadsö L, Stenström S (2016) Water vapor sorption and diffusivity in bark. Dry Technol 34:150–160. https://doi.org/10.1080/07373937.2015.1023310
27. Hoong YB, Paridah MT, Loh YF et al (2011) A new source of natural adhesive: Acacia mangium bark extracts co-polymerized with phenol-formaldehyde (PF) for bonding Mempisang (Annonaceae spp.) veneers. Int J Adhes Adhes 31:164–167. https://doi.org/10.1016/j.ijadhadh.2010.12.002
28. Jha K, Tyagi YK, Singh Yadav A (2018) Mechanical and thermal behaviour of biodegradable composites based on polycaprolactone with pine cone particle. Sadhana - Acad Proc Eng Sci 43:1–5. https://doi.org/10.1007/s12046-018-0822-1
29. Kain G, Barbu MC, Teischinger A et al (2012) Substantial bark use as insulation material. For Prod J 62:480–487. https://doi.org/10.13073/FPJ-D-12-00052.1
30. Kain G, Barbu MC, Hinterreiter S et al (2013a) Using bark as a heat insulation material. BioResources 8:3718–3731. https://doi.org/10.15376/biores.8.3.3718-3731
31. Kain G, Barbu MC, Petutschnigg A (2013b) Softwood bark for modern composites. Pro Ligno 9:460–468
32. Kain G, Güttler V, Barbu MC et al (2014) Density related properties of bark insulation boards bonded with tannin hexamine resin. Eur J Wood Wood Prod 72:417–424. https://doi.org/10.1007/s00107-014-0798-4
33. Kain G, Barbu MC, Richter K et al (2015) Use of tree bark as insulation material. For Prod J 65:16–25
34. Kain G(2016) Design of tree bark insulation boards: analysis of material, structure and property relationships
35. Kain G, Lienbacher B, Barbu MC et al (2018) Water vapour diffusion resistance of larch (Larix decidua) bark insulation panels and application considerations based on numeric modelling. Constr Build Mater 164:308–316. https://doi.org/10.1016/j.conbuildmat.2017.12.212
36. Khuntia T, Biswas S (2020) Characterization of a Novel Natural Filler from Sirisha Bark. J Nat Fibers 00:1–10. https://doi.org/10.1080/15440478.2020.1838997

37. Kolář V, Tichý M, Müller M (2019) Mechanical properties of polymeric composite based on pine seeds production residues. Manuf Technol 19:426–430. https://doi.org/10.21062/ujep/308.2019/a/1213-2489/MT/19/3/426
38. Korjenic A, Petránek V, Zach J, Hroudová J (2011) Development and performance evaluation of natural thermal-insulation materials composed of renewable resources. Energy Build 43:2518–2523. https://doi.org/10.1016/j.enbuild.2011.06.012
39. La Rosa AD, Recca A, Gagliano A et al (2014) Environmental impacts and thermal insulation performance of innovative composite solutions for building applications. Constr Build Mater 55:406–414. https://doi.org/10.1016/j.conbuildmat.2014.01.054
40. Mirski R, Kawalerczyk J, Dziurka D et al (2020) The application of oak bark powder as a filler for melamine-urea-formaldehyde adhesive in plywood manufacturing. Forests 11:1–12. https://doi.org/10.3390/f11121249
41. Pásztory Z, Mohácsiné IR, Gorbacheva G, Börcsök Z (2016) The utilization of tree bark. BioResources 11:7859–7888. https://doi.org/10.15376/biores.11.3.Pasztory
42. Pásztory Z, Ronyecz Mohácsiné I, Börcsök Z (2017) Investigation of thermal insulation panels made of black locust tree bark. Constr Build Mater 147:733–735. https://doi.org/10.1016/j.conbuildmat.2017.04.204
43. Pinto JRA, Sanches NB, Diniz MF et al (2018) Expanded perlite/cork fillers applied to aerospace insulation material. An Acad Bras Cienc 90:3197–3206. https://doi.org/10.1590/0001-3765201820170964
44. Réh R, Krišťák Ľ, Sedliačik J et al (2021) Utilization of birch bark as an eco-friendly filler in urea-formaldehyde adhesives for plywood manufacturing. Polym (Basel) 13:1–21. https://doi.org/10.3390/polym13040511
45. Rudenko BD (2010) Influence of structure on formation of properties of plates from the bark and secondary polyethylene. Mosc State Univ Bull 4:151–154
46. Sahin HT, Arslan MB (2011) Weathering performance of particleboards manufactured from blends of forest residues with red pine (Pinus brutia) wood. Maderas Cienc y Tecnol 13:337–346. https://doi.org/10.4067/S0718-221X2011000300009
47. Schiavoni S, D'Alessandro F, Bianchi F, Asdrubali F (2016) Insulation materials for the building sector: A review and comparative analysis. Renew Sustain Energy Rev 62:988–1011. https://doi.org/10.1016/j.rser.2016.05.045
48. Tsalagkas D, Börcsök Z, Pásztory Z (2019) Thermal, physical and mechanical properties of surface overlaid bark-based insulation panels. Eur J Wood Wood Prod 77:721–730. https://doi.org/10.1007/s00107-019-01436-5
49. TS EN 322 (1999a) Wood-based panels- Determination of moisture content. Turkish Standards Institute, Ankara, Turkey
50. TS EN 323 (1999b) Wood- Based panels- Determination of density. Turkish Standards Institute, Ankara, Turkey

51. TS EN 826 (2013) Thermal insulating products for building applications-Determination of compression behaviour. Turkish Standards Institute, Ankara, Turkey
52. TS EN 1604 (2013) Thermal insulating products for building application determination of dimensional stability under specified temperature and humidity conditions. Turkish Standards Institute, Ankara, Turkey
53. TS EN 1607 (2013) Thermal insulating products for building applications-Determination of tensile strength perpendicular to faces. Turkish Standards Institute, Ankara, Turkey
54. TS EN 1608 (2013) Thermal insulating products for building applications-Determination of tensile strength parallel to faces. Turkish Standards Institute, Ankara, Turkey
55. TS EN 13162 + A1 (2015) Thermal insulation products for buildings - Factory made mineral wool (MW) products - Specification. Turkish Standards Institute, Ankara, Turkey
56. TS EN 13163:2012 + A2 (2017) Thermal insulation products for buildings - Factory made expanded polystyrene (EPS) products - Specification. Turkish Standards Institute, Ankara, Turkey
57. TS EN 13164 + A1 (2015) Thermal insulation products for buildings - Factory made extruded polystyrene foam (XPS) products - Specification. Turkish Standards Institute, Ankara, Turkey
58. Tudor EM, Dettendorfer A, Kain G et al (2020a) Sound-absorption coefficient of bark-based insulation panels. Polym (Basel) 12. https://doi.org/10.3390/POLYM12051012
59. Tudor EM, Scheriau C, Barbu MC et al (2020b) Enhanced resistance to fire of the bark-based panels bonded with clay. Appl Sci 10. https://doi.org/10.3390/app10165594
60. Wesolowski A, Adams MA, Pfautsch S (2014) Insulation capacity of three bark types of temperate Eucalyptus species. For Ecol Manage 313:224–232. https://doi.org/10.1016/j.foreco.2013.11.015
61. Xing C, Zhang SY, Deng J, Wang S (2007) Investigation of the effects of bark fiber as core material and its resin content on three-layer MDF performance by response surface methodology. Wood Sci Technol 41:585–595. https://doi.org/10.1007/s00226-007-0129-6
62. Yemele MCN, Blanchet P, Cloutier A, Koubaa A (2008a) Effects of bark content and particle geometry on the physical and mechanical properties of particleboard made from black spruce and trembling aspen bark. For Prod J 58:48–56
63. Yemele MCN, Cloutier A, Diouf PN et al (2008b) Physical and mechanical properties of particleboard made from extracted black spruce and trembling aspen bark. For Prod J 58:38–46
64. Zhang Q, Lin X, Chen W et al (2020) Modification of rigid polyurethane foams with the addition of nano-SiO2 or lignocellulosic biomass. Polym (Basel) 12. https://doi.org/10.3390/polym12010106

Figures

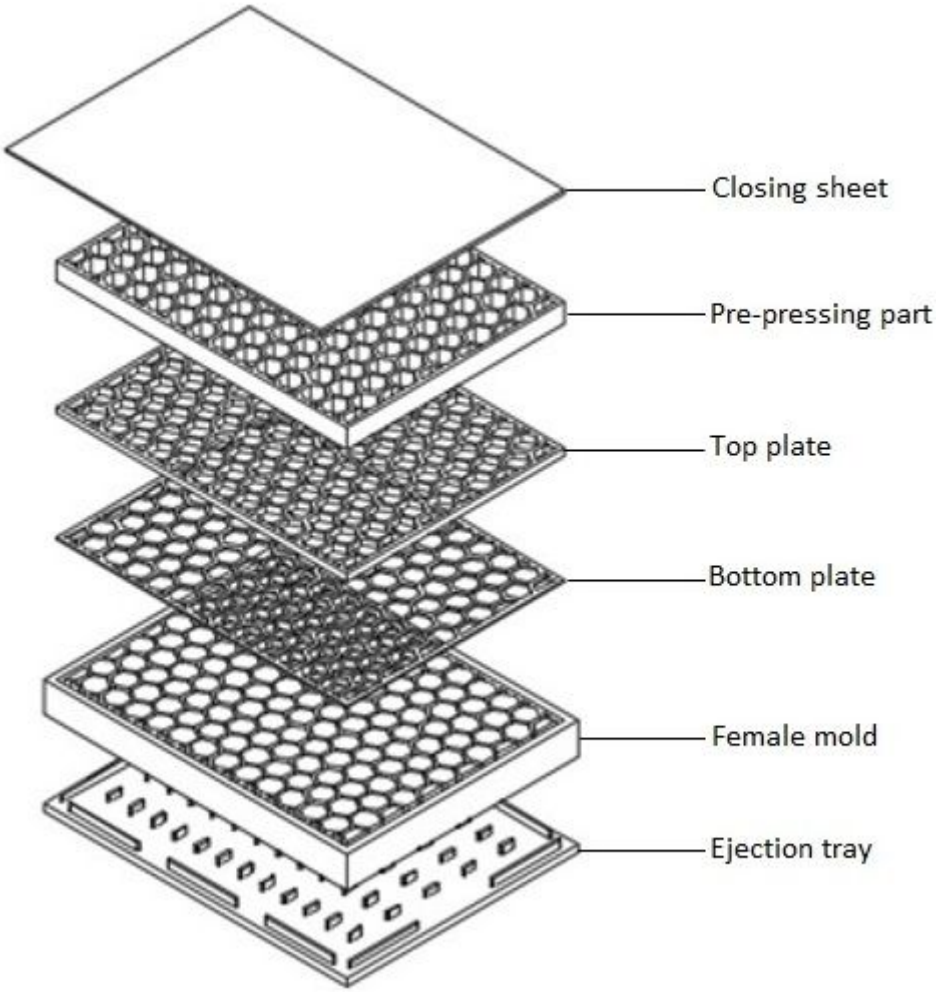

Figure 1

Parts of honeycomb-shaped aluminum alloy mold. It was adopted from Efe¸ (2022).

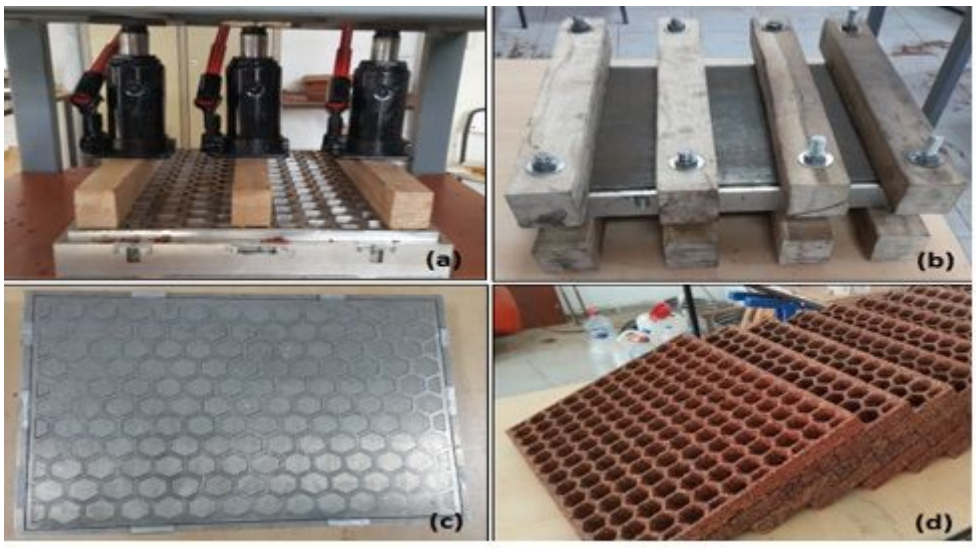

Figure 2

The apparatus used in the production of the core layer. Compression (a), fixation (b), closed mold (c), core layers (d). Figures were adopted from Efe¸ (2022).

Figure 3

Test setup of tensile strength parallel to the surface.

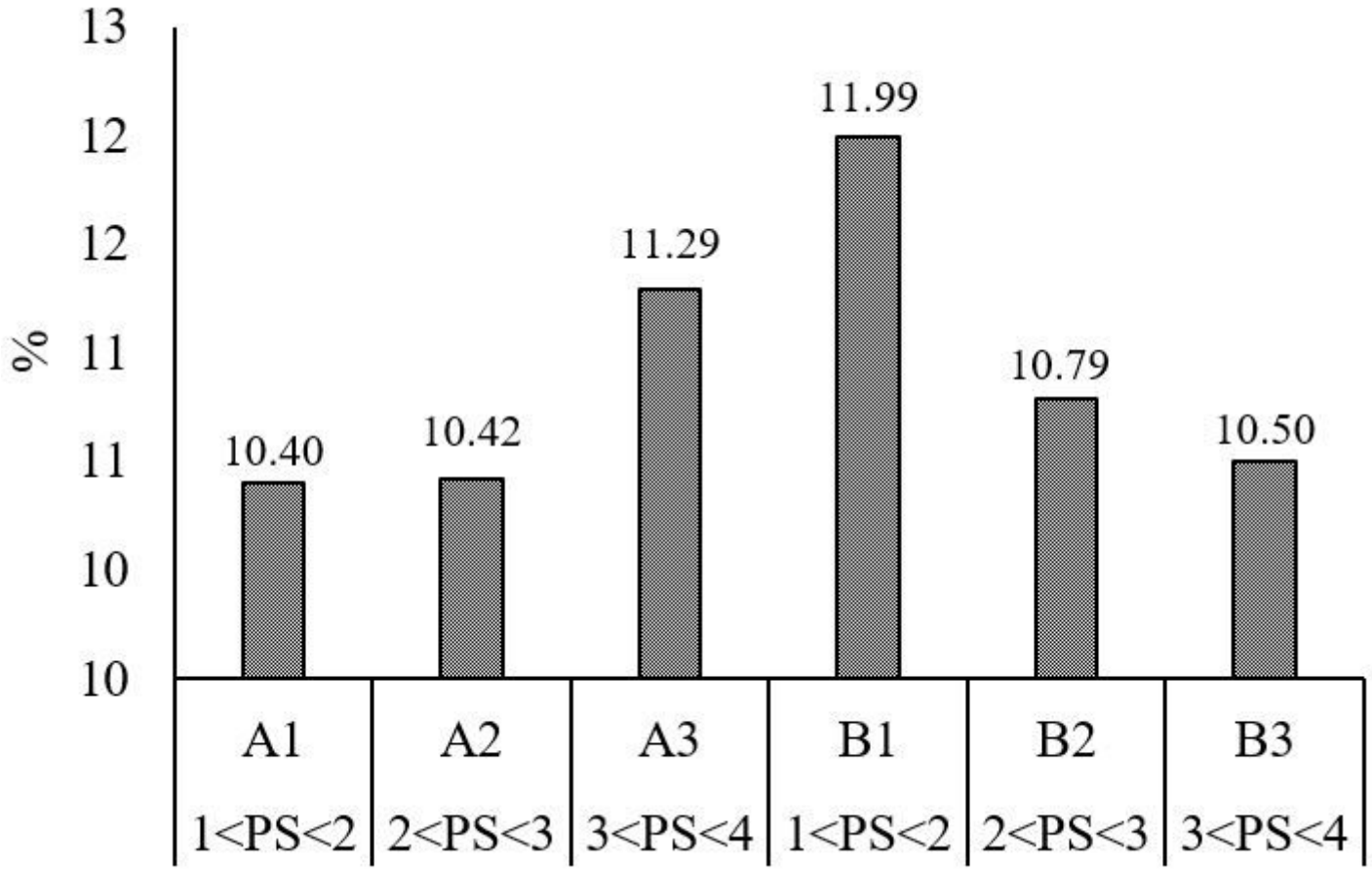

Figure 4

Particle size-MC relationships. Values were adopted from Efe, (2022).

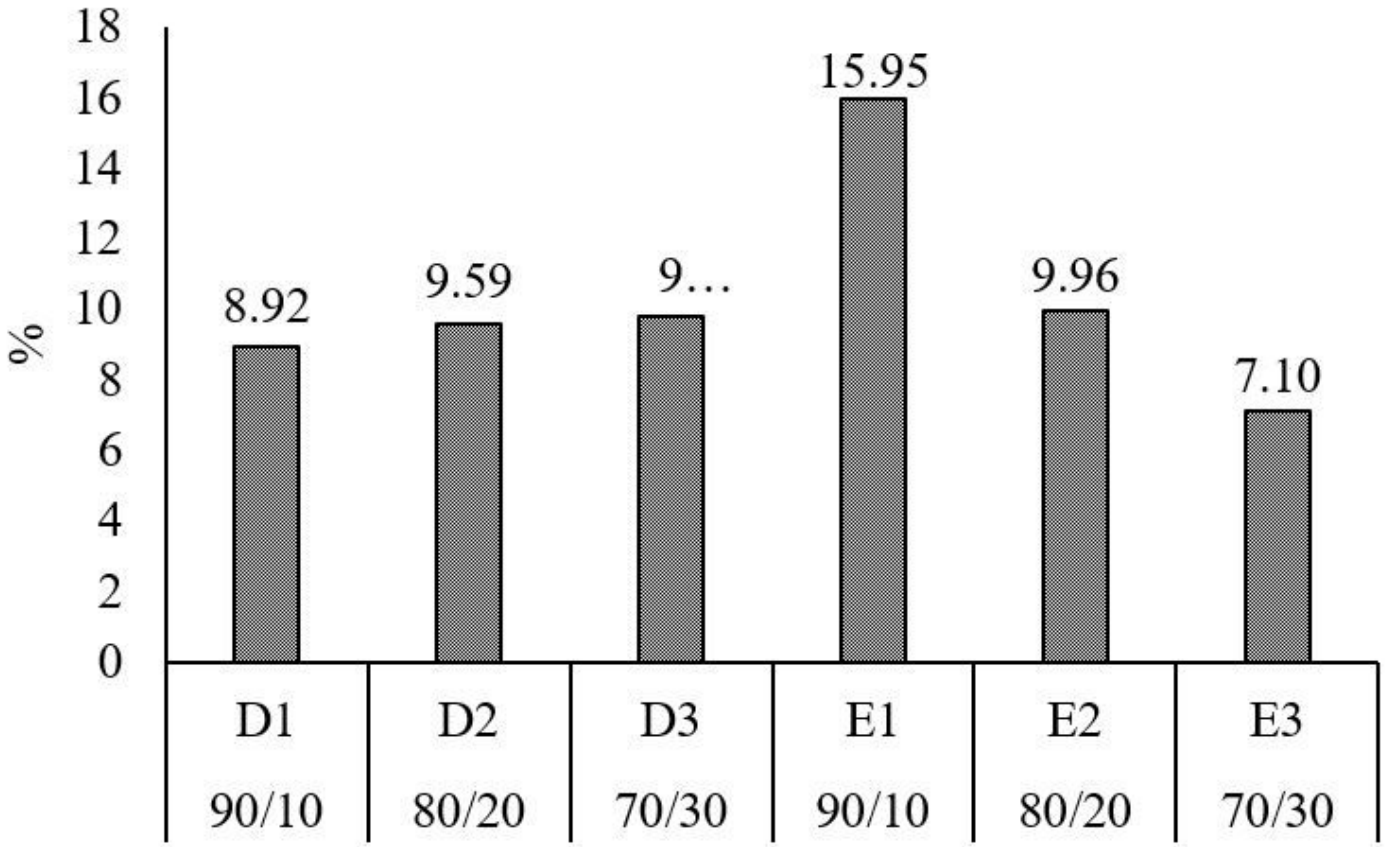

Figure 5

Perlite ratio-MC relationships. Values were adopted from Efe, (2022).

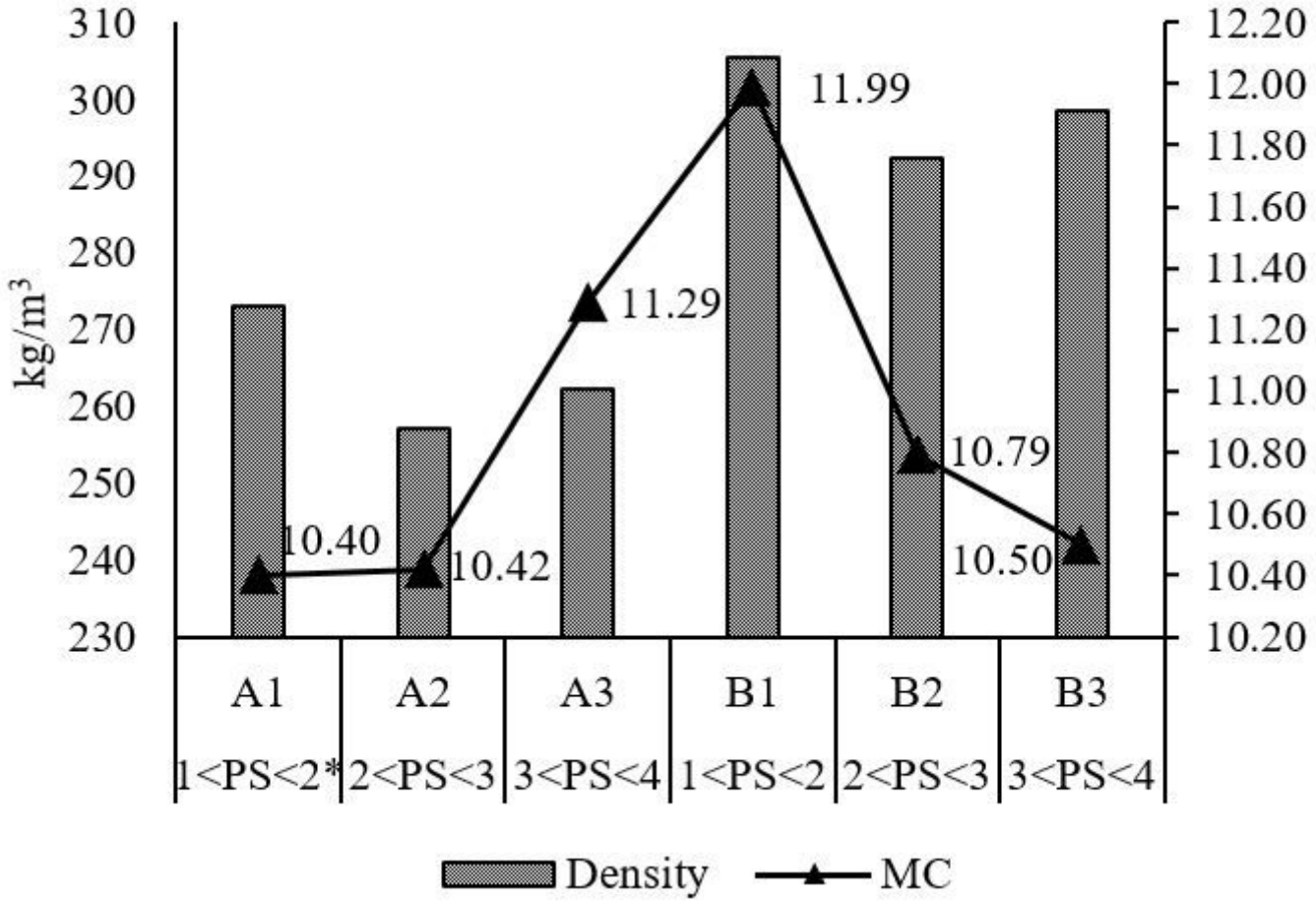

Figure 6

MC, density and particle size relationships. Values were adopted from Efe¸ (2022). **Particle size (mm).*

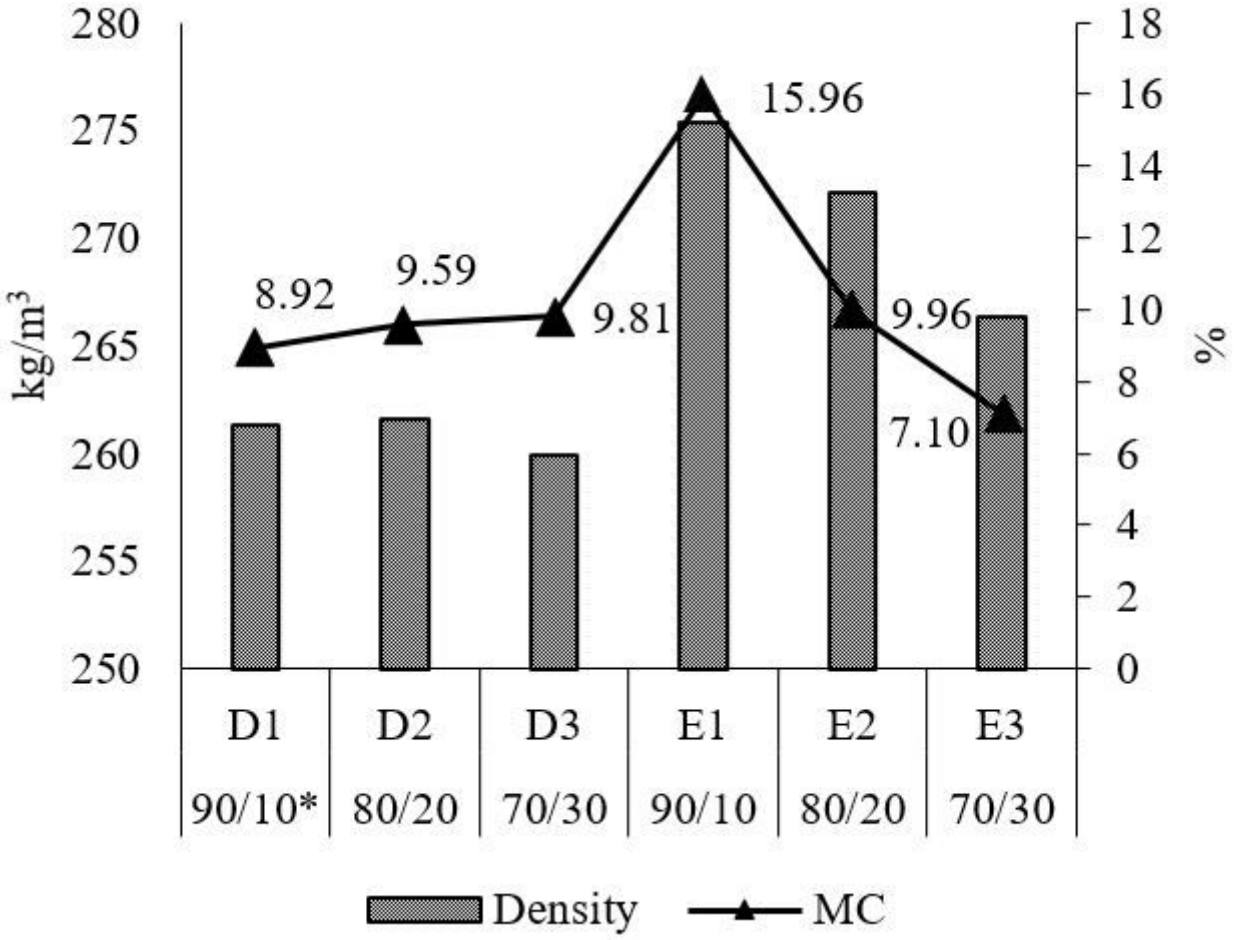

Figure 7

MC, density and perlite ratio relationships. Values were adopted from Efe¸ (2022). **Raw material/Perlite ratio (%).*

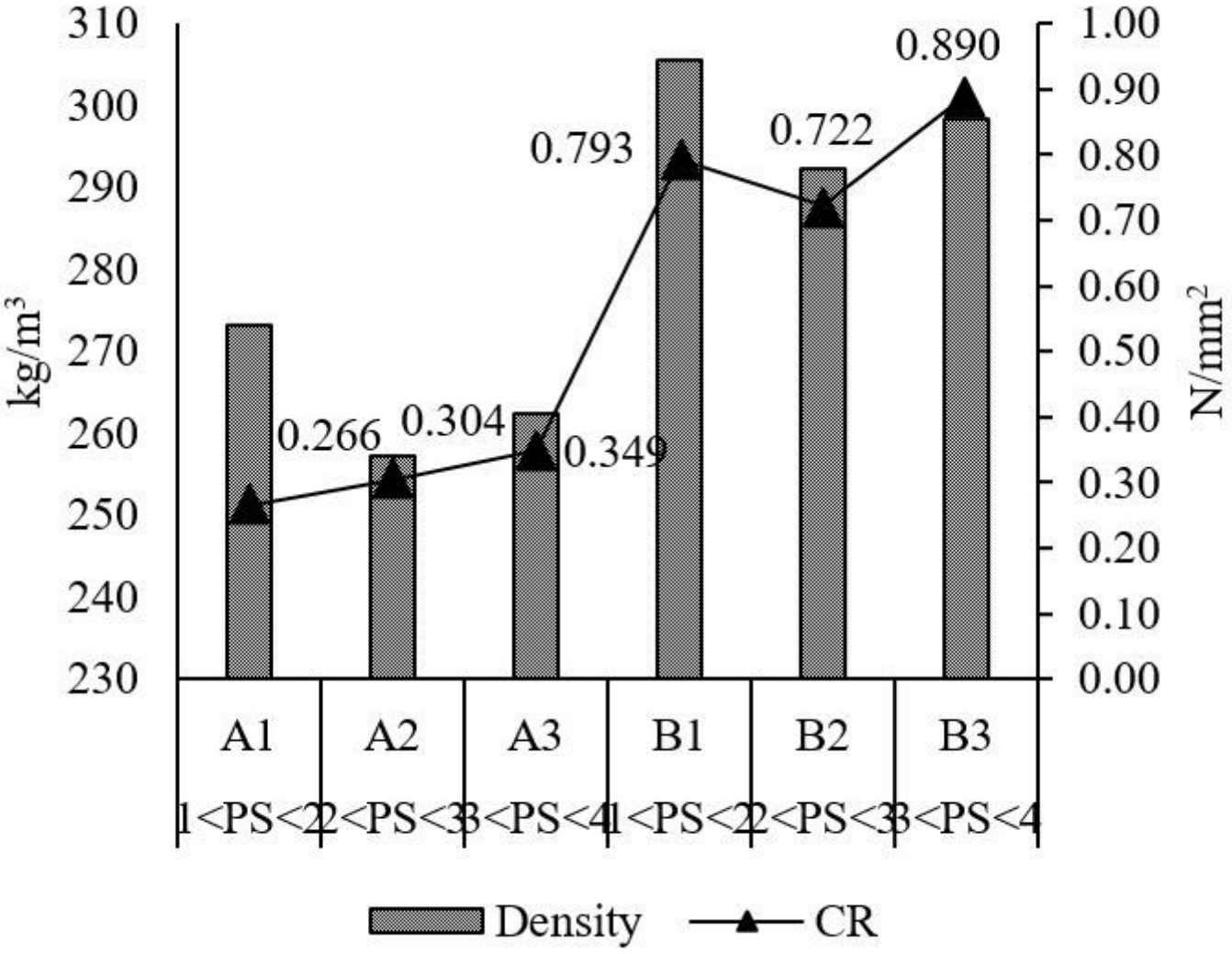

Figure 8

Particle size-density-compressive strength relationships.

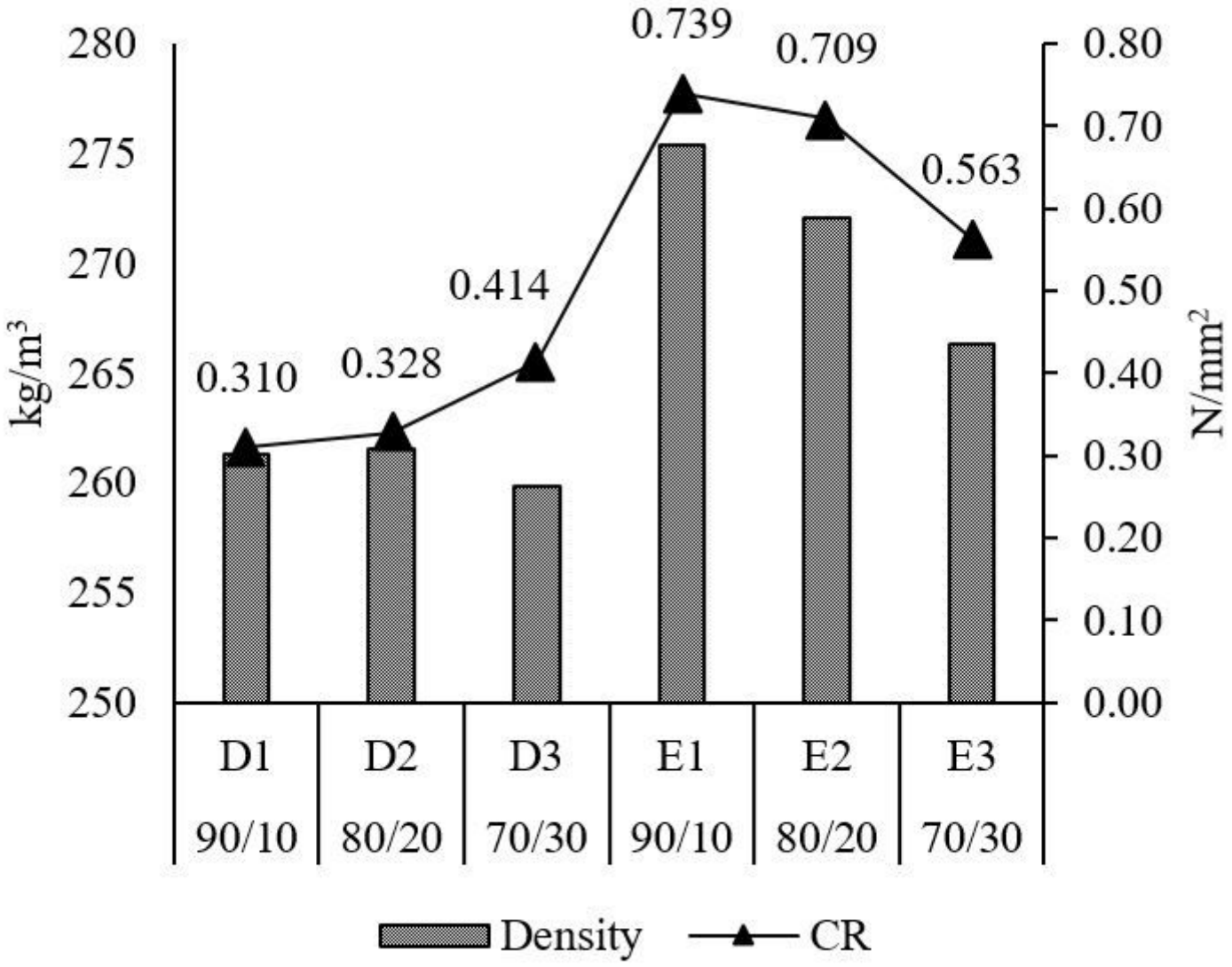

Figure 9

Perlite ratio-density-compressive strength relationships.

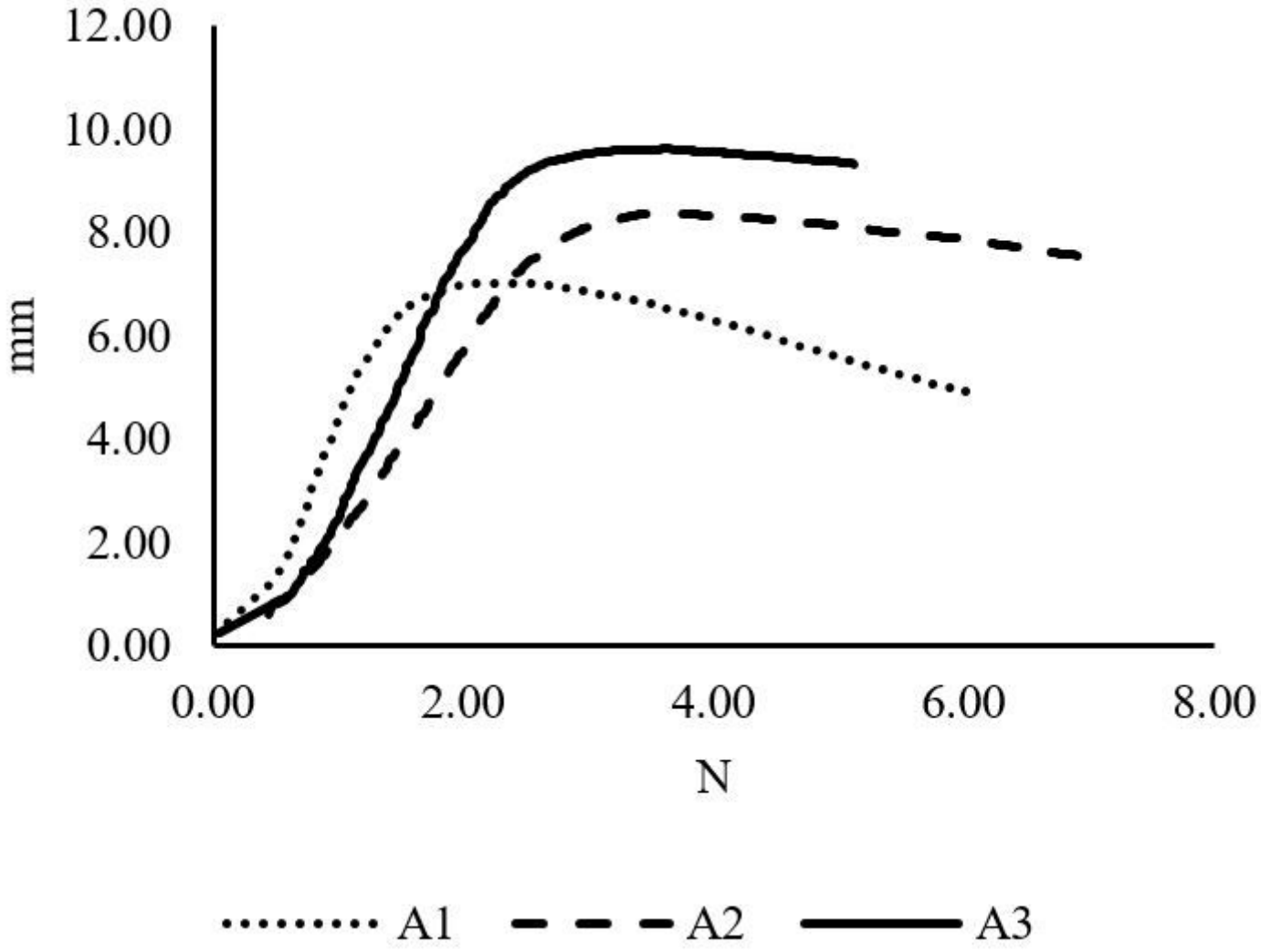

Figure 10

Force-deformation graph of group A materials.

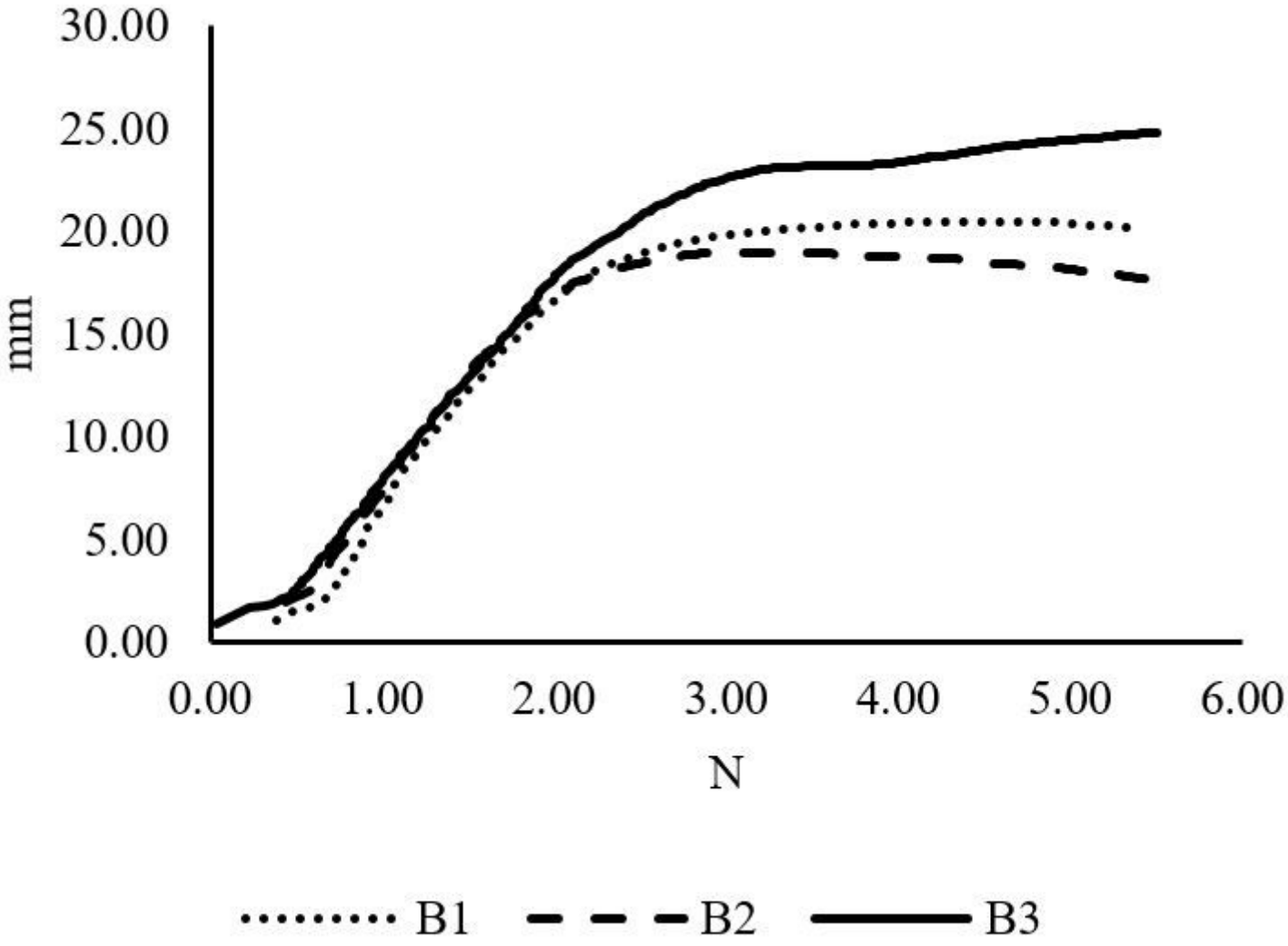

Figure 11

Force-deformation graph of group B materials.

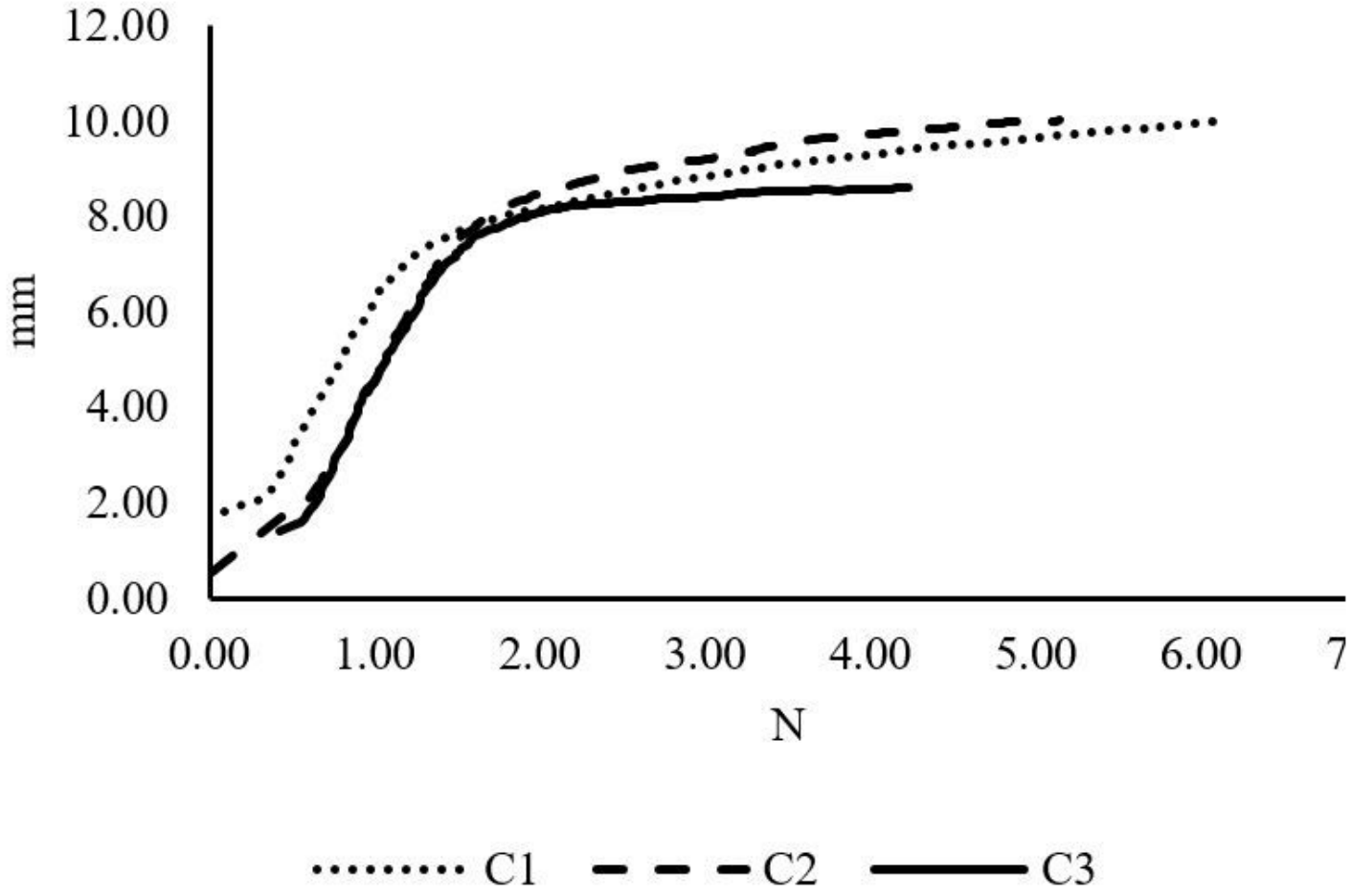

Figure 12

Force-deformation graph of group C materials.

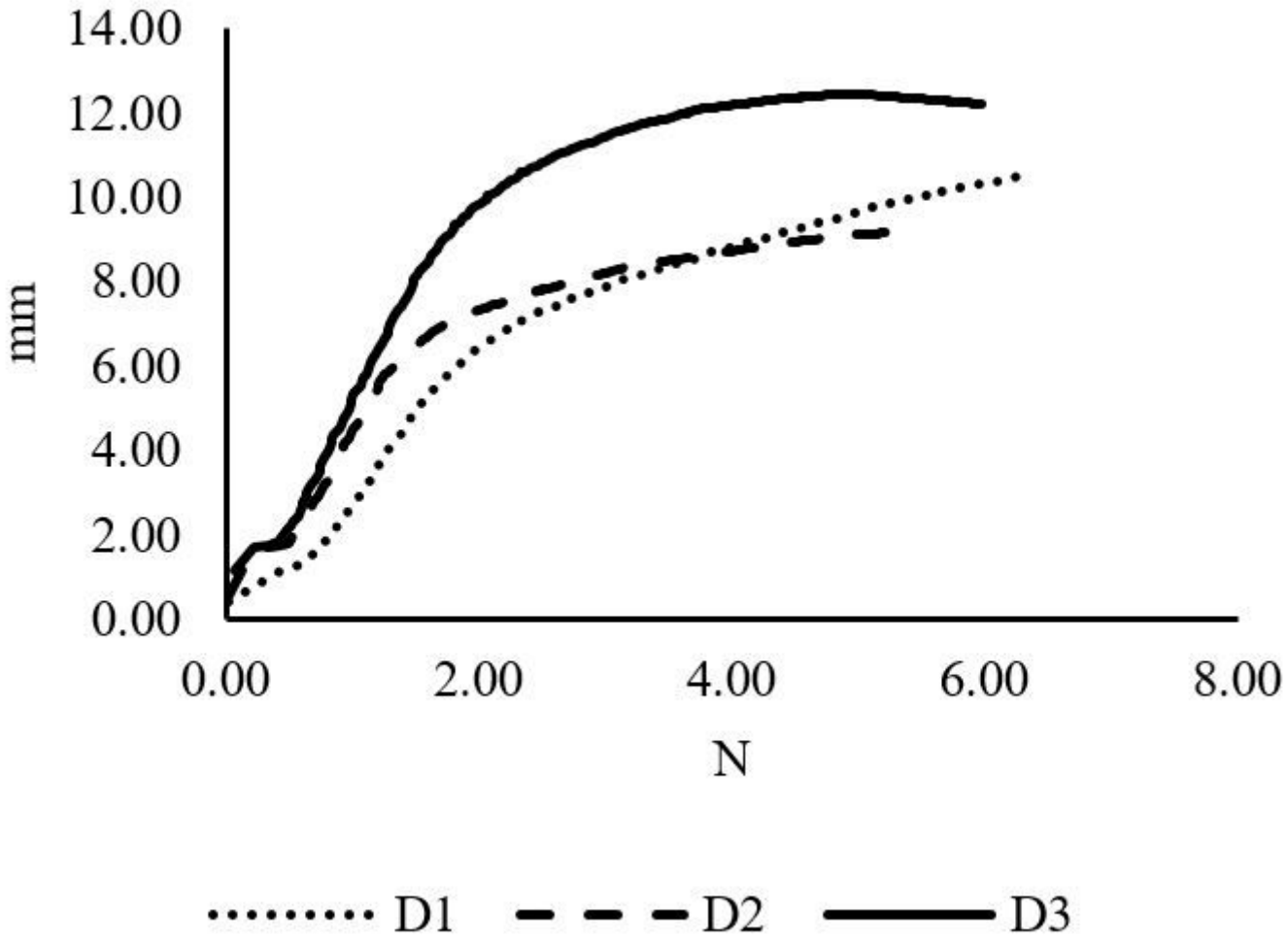

Figure 13

Force-deformation graph of group D materials.

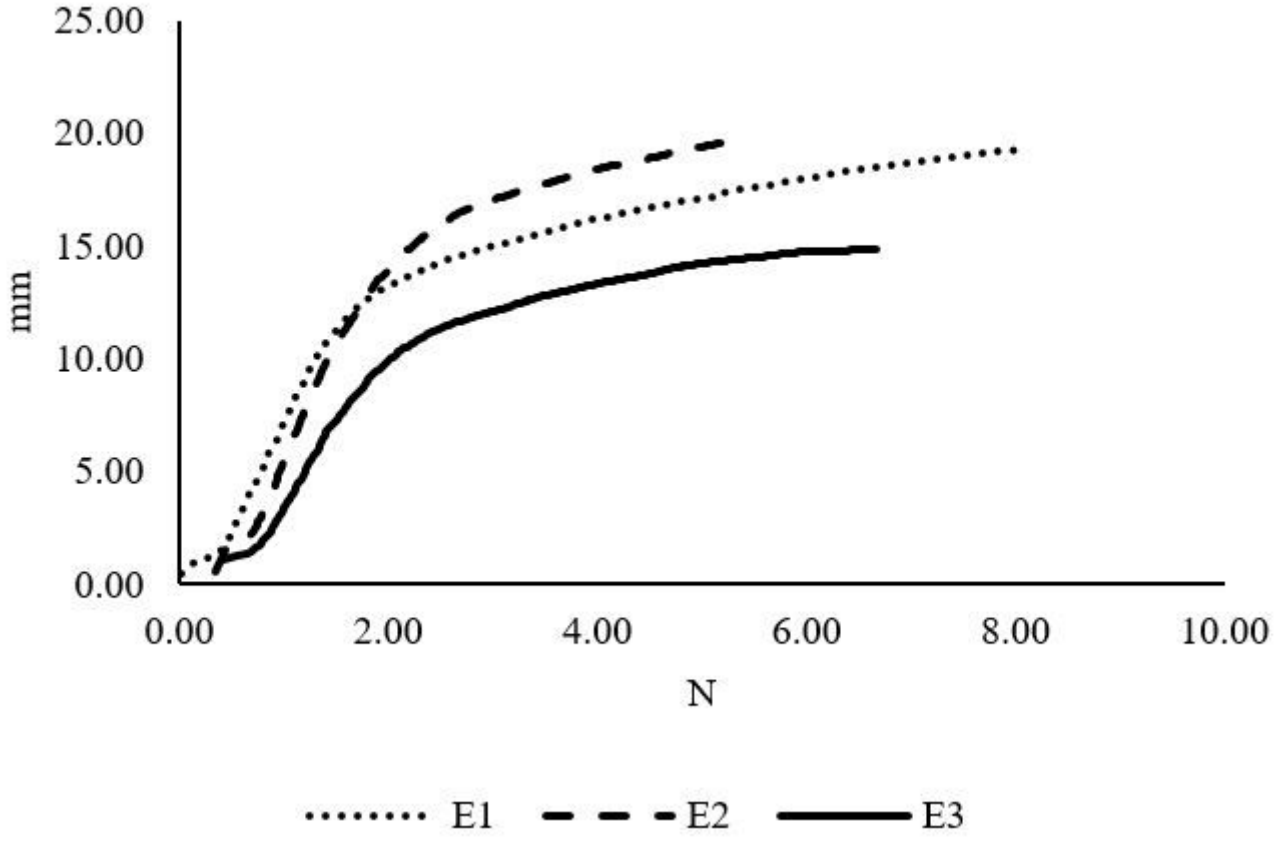

Figure 14

Force-deformation graph of group E materials.

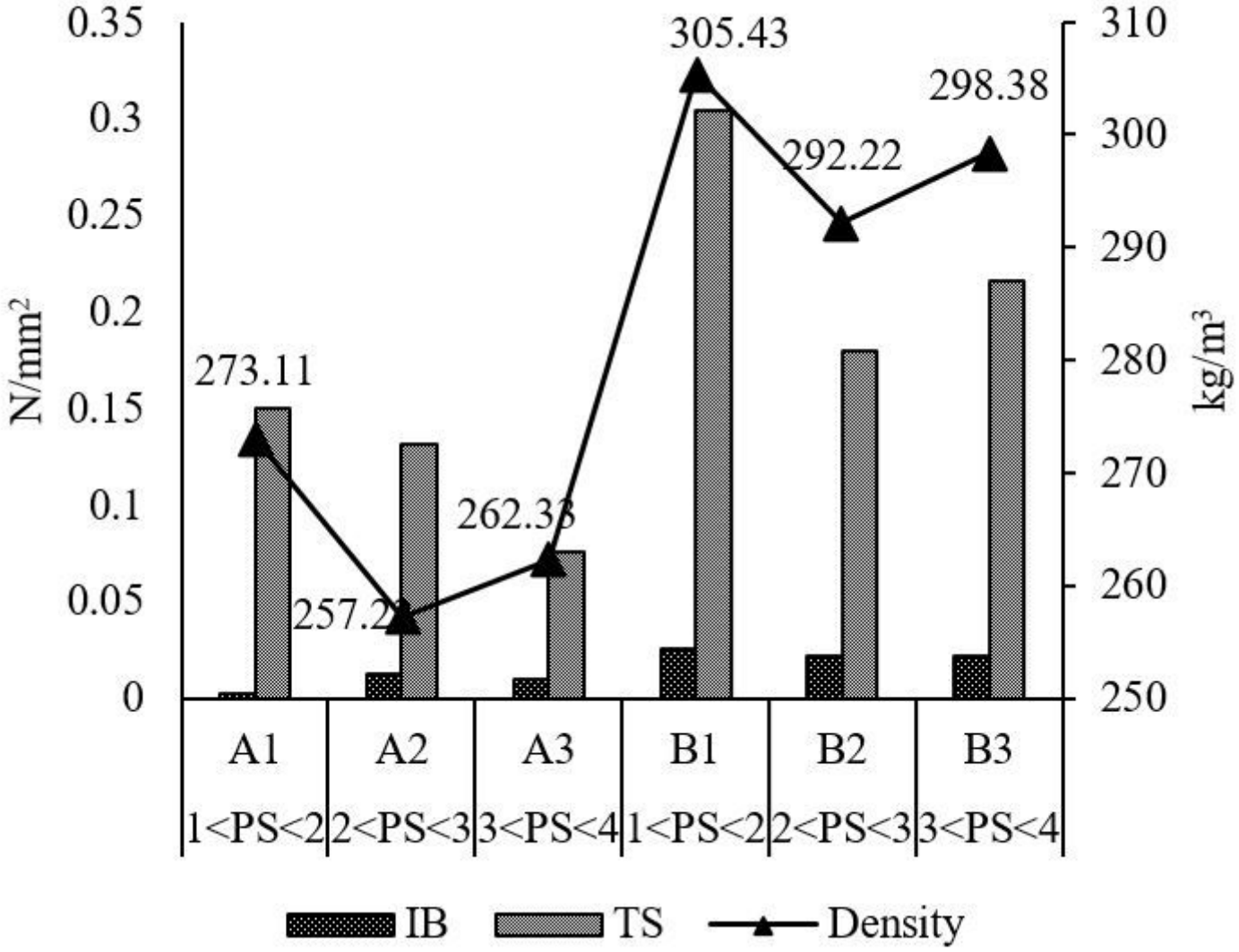

Figure 15

Particle size-density-IB-TS relationships.

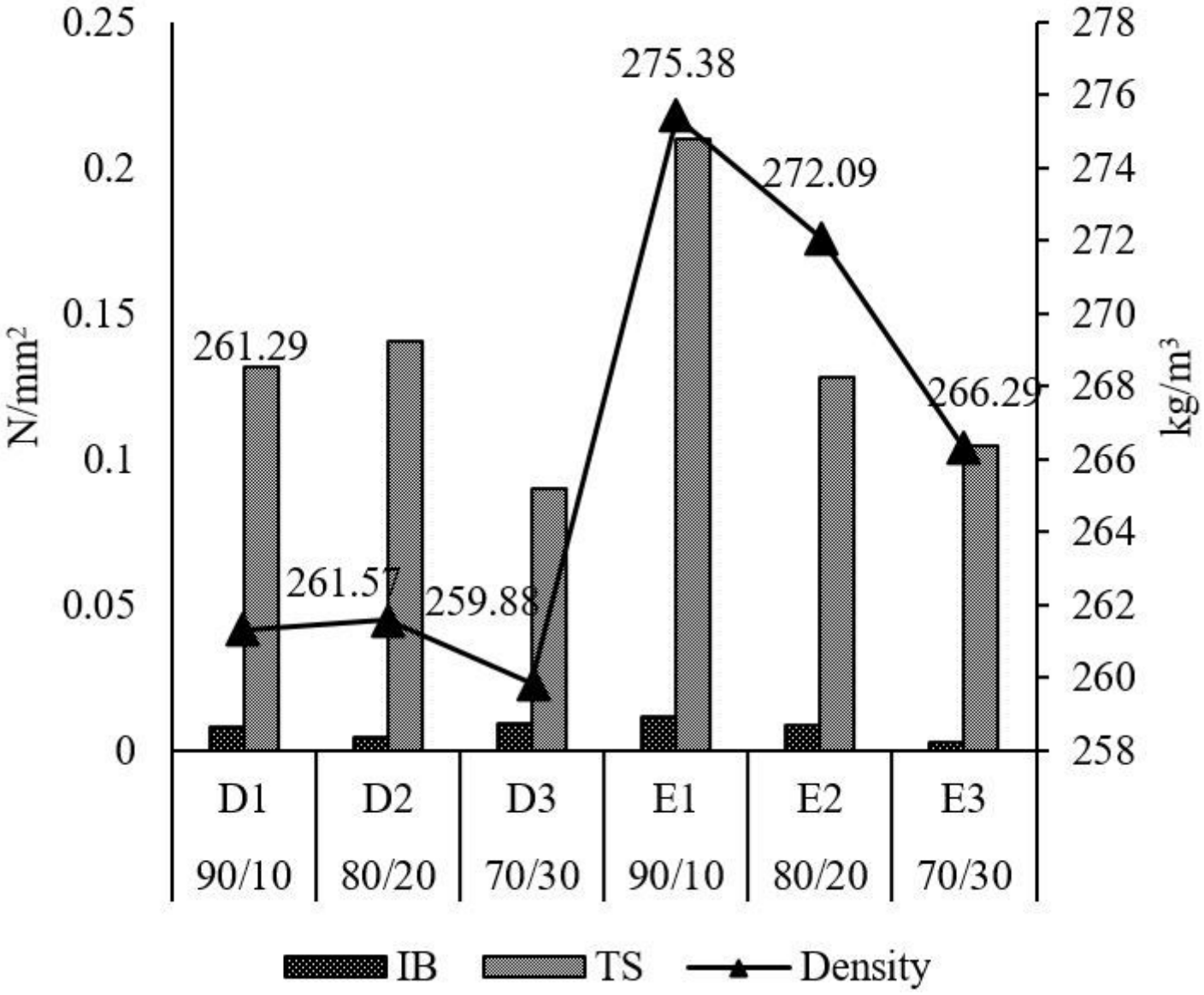

Figure 16

Perlite ratio-density-IB-TS relationships.